Mon. Not. R. astr. Soc. (1983) **203**, 1253–1268

Tidal interactions of disc galaxies

Ortwin E. Gerhard *Institute of Astronomy, Madingley Road, Cambridge CB3 0HA and Department of Theoretical Physics, Keble Road, Oxford OX1 3NP*
S. Michael Fall *Institute of Astronomy, Madingley Road, Cambridge CB3 0HA*

Received 1982 October 25; in original form 1982 January 13

Summary. We develop an analytic formalism to predict the cumulative effects of tidal encounters on disc galaxies in a variety of environments. The starting point is a modification of the standard impulse approximation that softens the interactions of overlapping galaxies. This is used to compute the changes in the stellar velocities parallel and perpendicular to the plane of a target disc during a single collision. A 20 000-body simulation shows that the corresponding energy changes are amplified only slightly by collective effects if the disc is stabilized by a halo. With this provision, we use the kinematic formulae and average over a realistic distribution of perturber masses and velocities. This excludes merging and adiabatic encounters but it includes graviational focusing and a proper weighting of the density profile in an aggregate. Our results show that most of the tidal heating is caused by interpenetrating collisions with velocities a few times higher than the circular velocities of the discs. The predicted changes in the epicyclic and vertical energies are then compared with observational data for a sample of galaxies in nearby groups and the Virgo cluster. We find that tidal heating cannot produce thick discs from thin discs and that it is unlikely to suppress spiral structure at a significant level. Tidal interactions might be important in the core of the Coma cluster but they appear to play a minor role in the evolution of most disc galaxies in their present environments over a Hubble time.

1 Introduction

The tidal distortions of galaxies during close encounters are often held responsible for changes in their kinematical and structural properties. Marchant & Shapiro (1977) have even suggested that mutual interactions in rich clusters might cause spiral and lenticular galaxies to heat up and thicken into elliptical galaxies. This proposal now seems unrealistic in view of the low rotational velocities and high central densities of ellipticals but it does raise the interesting question of what happens to disc galaxies that are repeatedly subjected to tidal perturbations. A partial answer is provided by the 1000-body simulations of Farouki & Shapiro (1981), which show that this process is unlikely to induce drastic changes in the morphology of galaxies over their lifetimes. To study the modest changes that would be missed with the low resolution of such simulations, we have developed an analytic treatment of the cumulative effects of tidal encounters on disc galaxies.

One motivation for this project stems from the recent photometry of edge-on disc galaxies by Burstein (1979c), Tsikoudi (1979, 1980) and van der Kruit & Searle (1981a, b). They have found changes in the shapes of the vertical density profiles at a few scale-heights that suggest a division of many of the discs into 'thin' and 'thick' components. One possibility is that thick discs are the parts of spheroidal bulges that have been flattened by the gravitational fields of their thin discs (Freeman 1980). Another possibility, considered in this paper, is that thick discs are the parts of the thin discs that have been heated by tidal encounters with other galaxies. Both suggestions are consistent with the prominence of thick discs in lenticular galaxies because they generally have large bulges and are generally located in high density environments where tidal encounters are expected to be frequent (Dressler 1980).

Another motivation for this project stems from the differences in spiral structure exhibited by galaxies of similar disc-to-bulge ratio. This is the basis for van den Bergh's (1976) system of classification, which includes a sequence of 'anaemic' galaxies between the sequences of normal spirals and lenticulars. Recent observations suggest that gas content alone does not determine the prominence of spiral structure and that some other factor is involved (Bothun & Sullivan 1980). Since gravitational instabilities are suppressed in hot discs, tidal heating might play a role in determining whether a disc galaxy takes on a spiral, anaemic or lenticular form. This possibility is in qualitative agreement with the correlation of these morphological types with their environment and it therefore requires a quantitative investigation. Tidal heating is also of interest in this context because tidal distensions are sometimes invoked as a driving mechanism for 'grand design' spiral patterns (Kormendy & Norman 1979; Toomre 1981).

2 A modified impulse approximation

We begin with the impulse approximation derived by Spitzer (1958) in his study of the disruption of open clusters by passing clouds. This is based on the assumption that the velocity of a perturber $\mathbf{v}_p$ is high enough that the orbit is nearly straight and that the stars in the target can be considered motionless during the encounter. It is also assumed that the pericentre of the perturber $\mathbf{p}$ is large enough that the tidal force on a star can be approximated to first order in r_s/p, where $\mathbf{r}_s$ is the position of the star relative to the centre of the target. Then the instantaneous change in the velocity of the star induced by the encounter is

$$\delta \mathbf{v}_s \simeq \frac{2GM_p}{v_p p^2} [2(\mathbf{r}_s \cdot \mathbf{e}_p)\mathbf{e}_p + (\mathbf{r}_s \cdot \mathbf{e}_v)\mathbf{e}_v - \mathbf{r}_s] \tag{1}$$

where $\mathbf{e}_p$ and $\mathbf{e}_v$ are unit vectors parallel to $\mathbf{p}$ and $\mathbf{v}_p$ respectively, M_p is the mass of the perturber and G is the gravitational constant. This equation, with various modifications, has been applied to the tidal interactions of galaxies by Alladin (1965), Richstone (1975, 1976), Knobloch (1976, 1978) and others.

For large impact parameters and slow encounter velocities, $\delta \mathbf{v}_s$ must vanish because stars in the target react adiabatically to the perturbation. As Spitzer (1958) showed, this happens when v_p/p is less than some characteristic frequency for stellar motions within the target. The critical frequency should depend on the position of the star under consideration, the mass distribution in the two galaxies and, to some extent, on their relative orbit. We assume that all of this dependence scales as the Roche radius in the following way:

$$p_{\rm max}/v_{\rm p} \simeq 5\,(M_{\rm p}/M_{\rm t})^{1/3}(r_{\rm s}/v_{\rm e5}) \tag{2}$$

where M_t is the mass of the target galaxy and v_{e5} is the escape velocity of the two galaxies at the distance $5(M_p/M_t)^{1/3}r_s$. The coefficient 5 in equation (2) is consistent with the restricted three-body calculations of Toomre & Toomre (1972) and the self-gravitating N-body simulations of Gerhard (1981) for interacting disc galaxies. Our final results are not sensitive to small variations in this numerical factor.

Equation (1) also breaks down for small impact parameters because the galaxies then overlap and may even merge if their relative velocity is low. The validity of the standard impulse approximation for relatively slow and close encounters that do not lead to merging was studied by Dekel, Lecar & Shaham (1980) through N-body simulations. Their results can be summarized by the condition

$$p^2 v_{\rm p} \gtrsim 2.7\,(GM_{\rm p}^2/M_{\rm t})^{1/2} r_{\rm Ht}^{3/2}\,\nu_{\rm c}^{-1} \tag{3}$$

where ν_c has a value near unity and a weak dependence on the ratio of the rms to the half-mass radius r_{Ht} of the target galaxy has been ignored. This criterion is to be compared with the condition for merging, which has been derived from a variety of N-body experiments and summarized by Aarseth & Fall (1980) in the expression

$$\frac{p^2}{[2\,(r_{\rm Ht}+r_{\rm Hp})]^2}+\frac{v_{\rm p}^2}{[1.16\,v_{\rm e}(p)]^2}\leqslant 1 \tag{4}$$

where $v_e(p)$ is the escape velocity at pericentre and r_{Hp} denotes the half-mass radius of the perturber galaxy.

The regimes defined by equations (2) to (4) are shown in Fig. 1 for the case that the target and perturber have equal scale-radii and masses. For the escape velocity we have used the expression

$$v_{\rm e}^2(p) \simeq 2G\,(M_{\rm t}+M_{\rm p})\,(p^2+\epsilon_{\rm t}^2+\epsilon_{\rm p}^2)^{-1/2} \tag{5}$$

as a convenient approximation for two overlapping Plummer spheres with length scales related by $\epsilon = r_H/1.3$. In comparison with the exact expression, equation (5) is accurate to about 15 per cent in the worst case, for which $p \simeq 0$ and $\epsilon_t \simeq \epsilon_p$. In what follows, we exclude bound and merging orbits by using condition (4) or $v_p \geqslant v_e(p)$, whichever is appropriate. We are thus concerned with encounters in the hatched region in Fig. 1 where they are often interpenetrating. From this it is clear that equation (1) requires some improvement over a significant part of the pv_p-plane.

To obtain a simple modification of the standard impulse approximation, we assume that the two galaxies can be represented by rigid Plummer spheres. The total acceleration exerted by the perturber at position $\mathbf{r}_p$ on a star at position $\mathbf{r}_s$ in the target is then

$$\mathbf{f}_{\rm tot}=\frac{GM_{\rm p}(\mathbf{r}_{\rm p}-\mathbf{r}_{\rm s})}{(|\mathbf{r}_{\rm p}-\mathbf{r}_{\rm s}|^2+\epsilon_{\rm p}^2)^{3/2}}. \tag{6}$$

For a perturber on a straight line orbit, given by $\mathbf{r}_p = \mathbf{p} + \mathbf{v}_p t$ with $\mathbf{p}\cdot\mathbf{v}_p = 0$, the corresponding change in the velocity of the star is

$$\delta\mathbf{v}_{\rm tot}=\int_{-\infty}^{+\infty}dt\,\mathbf{f}_{\rm tot}(t)=\frac{2GM_{\rm p}}{v_{\rm p}}\left[\frac{(\mathbf{p}-\mathbf{r}_{\rm s})+(\mathbf{r}_{\rm s}\cdot\mathbf{e}_{\rm v})\mathbf{e}_{\rm v}}{|\mathbf{r}_{\rm s}-\mathbf{p}|^2+\epsilon_{\rm p}^2-(\mathbf{r}_{\rm s}\cdot\mathbf{e}_{\rm v})^2}\right]. \tag{7}$$

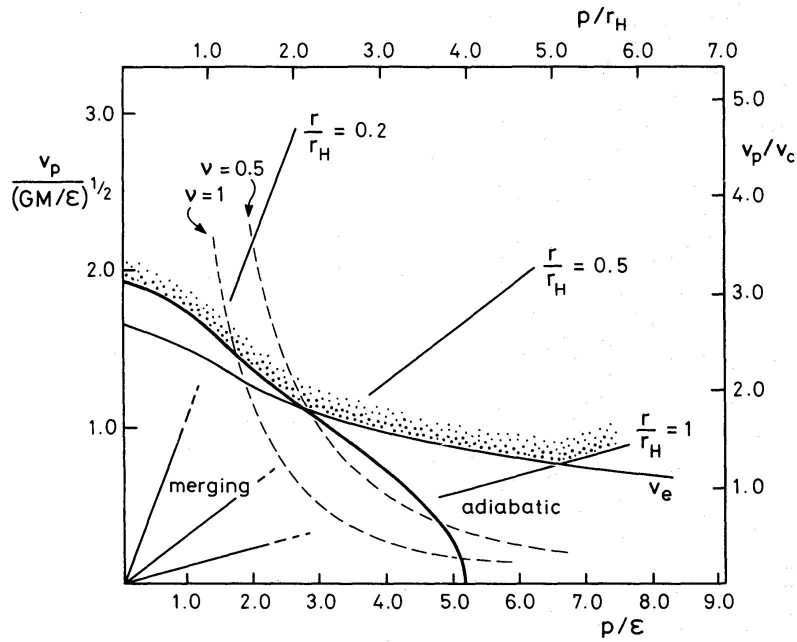

Figure 1. Encounter regimes in the pericentre–velocity plane for identical targets and perturbers. The condition specified by equation (2) for an adiabatic response is shown by the diagonal lines for three positions within the target. Equation (3) for the validity of the impulse approximation is plotted as the dashed lines for two values of the critical parameter ν_c. The bold line is the condition for merging specified by equation (4) and the nearby weak line shows the escape velocity approximated by equation (5). Contributions to the energy changes from the region below the stippling are excluded in the averages over encounters.

The tidal change with respect to the centre of the target is obtained by subtracting the analogous quantity after integration over its density profile; thus

$$\delta \mathbf{v}_s = \frac{2GM_p}{v_p} \int d^3\mathbf{r}'_s \left[\frac{(\mathbf{p}-\mathbf{r}'_s)+(\mathbf{r}'_s\cdot\mathbf{e}_v)\mathbf{e}_v}{|\mathbf{r}'_s-\mathbf{p}|^2+\epsilon_p^2-(\mathbf{r}'_s\cdot\mathbf{e}_v)^2}\right]\left[\delta(\mathbf{r}_s-\mathbf{r}'_s)-\frac{3\epsilon_t^2}{4\pi(|\mathbf{r}'_s|^2+\epsilon_t^2)^{5/2}}\right]. \tag{8}$$

This expression is still too complicated for our applications and we therefore make some simplifying approximations.

For distant encounters, the integrand of equation (8) can be expanded in powers of $r'_s/p \sim \epsilon_p/p \sim \epsilon_t/p$ and from the first-order terms we recover equation (1). The opposite limit gives

$$\delta \mathbf{v}_s \simeq \frac{2GM_p}{v_p\,[r_s^2+\epsilon_p^2-(\mathbf{r}_s\cdot\mathbf{e}_v)^2]}\,[(\mathbf{r}_s\cdot\mathbf{e}_v)\mathbf{e}_v-\mathbf{r}_s] \tag{9}$$

to zeroth order in p/r_s and p/ϵ. Without introducing any errors larger than the ones already made, we set $(\mathbf{r}_s\cdot\mathbf{e}_v)^2 = {}^1\!/\!_3 r_s^2$, the average over all possible orientations of $\mathbf{r}_s$ and $\mathbf{e}_v$. Interpolating between equations (1) and (9) gives our final expression

$$\delta \mathbf{v}_s \simeq \frac{2GM_p}{v_p\,(p^2+\epsilon_p^2+{}^2\!/\!_3 r_s^2)}\left[\frac{2p^2}{(p^2+\epsilon_p^2+{}^2\!/\!_3 r_s^2)}(\mathbf{r}_s\cdot\mathbf{e}_p)\mathbf{e}_p+(\mathbf{r}_s\cdot\mathbf{e}_v)\mathbf{e}_v-\mathbf{r}_s\right]. \tag{10}$$

This formula is convergent for small impact parameters and it implies that stars with $\mathbf{r}_s$ parallel to $\mathbf{p}$ are pulled inwards for almost head-on collisions. Equation (10) still breaks down for small relative velocities but these are excluded in the remainder of our treatment.

The application of the formulae above to disc galaxies might be questionable if they were entirely self-gravitating bodies. However, the shapes and amplitudes of their rotation curves imply that at least half of the mass within their Holmberg radii is dark and the inferred haloes are usually assumed to be roughly spherical (see, for example, Fall & Efstathiou 1980). It therefore seems reasonable to apply equation (10) to the tidal interactions of disc galaxies with the following conversion factors:

$$v_c^2 = GM/2r_H, \qquad r_H = 1.3\epsilon \tag{11}$$

where v_c is the characteristic circular velocity, M is the mass and r_H is the median (half-mass) radius of the combined disc–halo system. The first equation is not sensitive to the detailed form of the density profile and the second equation relates the two length-scales for a Plummer model. For convenience, we have labelled Fig. 1 with both sets of variables, (M, ϵ) and (v_c, r_H).

3 Changes in a single encounter

We first consider the motions of stars parallel to the plane of the target disc. In the epicyclic approximation, the radial and azimuthal velocities with respect to the circular velocity at the instantaneous position of a star, u and v, satisfy the well-known equations of motion (Lindblad 1959)

$$\dot{u} - 2\Omega v = 0, \qquad \dot{v} + (\kappa^2/2\Omega)u = 0 \tag{12}$$

where $\Omega(R)$ and $\kappa(R)$ are respectively the circular and epicyclic frequencies at the radial position R in the disc. A constant of the unperturbed motion is the epicyclic energy per unit mass, defined by

$$E_e \equiv \tfrac{1}{2}u^2 + \tfrac{1}{2}(2\Omega/\kappa)^2 v^2. \tag{13}$$

An average over the amplitudes and phases of the epicycles at fixed R gives

$$\langle E_e \rangle = \langle u^2 \rangle = (2\Omega/\kappa)^2 \langle v^2 \rangle. \tag{14}$$

A similar operation just after an impulsive encounter gives the average change in the epicyclic energy

$$\langle \delta E_e \rangle = \tfrac{1}{2}(\delta u)^2 + \tfrac{1}{2}(2\Omega/\kappa)^2(\delta v)^2 \tag{15}$$

where δu and δv are the radial and azimuthal components of $\delta \mathbf{v}_s$.

We are also interested in the motions of stars perpendicular to the plane of the target disc. For a plane-stratified gravitational system, the time-independent virial theorem is

$$E_z = W_z + T_z = 3T_z = \tfrac{3}{2}\langle w^2 \rangle \tag{16}$$

where T_z, W_z, E_z denote the kinematic, potential and total energy in vertical (z) motions per unit mass, w is the vertical component of the velocity and the averages are over the amplitudes and phases of the oscillations (Camm 1967). Equation (16) differs from the ordinary virial theorem in that the potential energy must be reckoned positive for a bound system but the kinetic energy is still given by $T_z = \tfrac{1}{2}\langle w^2 \rangle$. Just after an encounter, the average change in the vertical energy is therefore

$$\langle \delta E_z \rangle = \tfrac{1}{2}(\delta w)^2 \tag{17}$$

where δw is the vertical component of $\delta \mathbf{v}_s$.

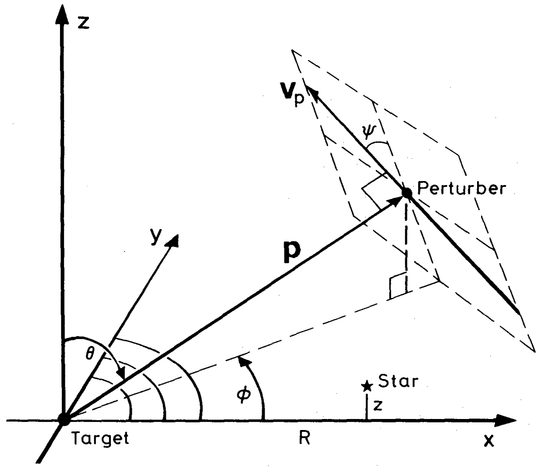

Figure 2. Coordinate system used in the averages over encounters. The target disc lies in the xy-plane and the location of a star is specified by (R, ϕ, z). With respect to this position, the pericentre and velocity of a perturber are specified completely by (p, v_p, θ, ψ).

To compute the velocity perturbations $\delta \mathbf{v}_s = (\delta u, \delta v, \delta w)$ explicitly, we use the results of the previous section and introduce the coordinate system depicted in Fig. 2. The polar angle θ and the azimuthal angle ψ specify the orientation of the velocity of the perturber $\mathbf{v_p}$ with respect to the symmetry axis of the target disc and the cylindrical coordinates $r_s = (R, \phi, z)$ denote the position of a star in the disc. Without loss of generality, the origin of the azimuthal angle ϕ is taken to be the projection of the pericentre of the perturber $\mathbf{p}$ on to the plane of the target disc. The unit vectors in the directions of $\mathbf{p}$ and $\mathbf{v_p}$ are then

$$\mathbf{e_p} = \begin{pmatrix} \sin\theta\cos\phi \\ \sin\theta\sin\phi \\ \cos\theta \end{pmatrix}, \qquad \mathbf{e_v} = \begin{pmatrix} -\sin\psi\sin\phi - \cos\psi\cos\theta\cos\phi \\ \sin\psi\cos\phi - \cos\psi\cos\theta\sin\phi \\ \cos\psi\sin\theta \end{pmatrix} \tag{19}$$

and they satisfy $\mathbf{e_p} \cdot \mathbf{e_v} = 0$ as required. Substituting these expressions into equation (10) and neglecting terms of order z/R gives

$$\begin{pmatrix} \delta u \\ \delta v \\ \delta w \end{pmatrix} = \Lambda \left[\Pi \sin\theta\cos\phi\, \mathbf{e_p} - (\sin\psi\sin\phi + \cos\psi\cos\theta\cos\phi)\, \mathbf{e_v} - \begin{pmatrix} 1 \\ 0 \\ 0 \end{pmatrix} \right] \tag{19}$$

where

$$\Lambda \equiv \frac{2GM_pR}{v_p(p^2 + \epsilon_p^2 + \tfrac{2}{3}R^2)}, \qquad \Pi \equiv \frac{2p^2}{p^2 + \epsilon_p^2 + \tfrac{2}{3}R^2}. \tag{20}$$

Averaging over ϕ at fixed R, we obtain after some lengthy manipulations

$$\langle \delta u \rangle = \tfrac{1}{2}\Lambda(\Pi\sin^2\theta - \cos^2\psi\sin^2\theta - 1) \tag{21}$$

$$\langle \delta v \rangle = \langle \delta w \rangle = 0 \tag{22}$$

$$\langle (\delta u)^2 \rangle = \Lambda^2 [\tfrac{3}{8}\Pi^2\sin^4\theta + \tfrac{1}{4}\Pi\sin^2\theta(\sin^2\psi + 3\cos^2\psi\cos^2\theta - 4) + \tfrac{3}{8}(\sin^4\psi + \cos^4\psi\cos^4\theta + 2\sin^2\psi\cos^2\psi\cos^2\theta + \tfrac{8}{3}\cos^2\psi\sin^2\theta)] \tag{23}$$

$$\langle (\delta v)^2 \rangle = \Lambda^2 [\tfrac{1}{8}\Pi^2\sin^4\theta + \tfrac{1}{4}\Pi\sin^2\theta(\cos^2\psi\cos^2\theta - \sin^2\psi) + \tfrac{1}{8}(\sin^4\psi + \cos^4\psi\cos^4\theta + 2\sin^2\psi\cos^2\psi\cos^2\theta)] \tag{24}$$

$$\langle(\delta w)^2\rangle = \Lambda^2 [\tfrac{1}{2}\Pi^2 \sin^2\theta\cos^2\theta - \Pi\cos^2\psi\sin^2\theta\cos^2\theta + \tfrac{1}{2}\sin^2\theta\,(\sin^2\psi\cos^2\psi + \cos^4\psi\cos^2\theta)]. \quad (25)$$

The fact that $\langle\delta u\rangle$ is non-zero reflects the initiation of radial streaming motions by the encounter. As equation (15) shows, this makes no contribution to the epicyclic energy in the approximation that the unperturbed stellar orbits have random phases in an axisymmetric disc. The vanishing of $\langle\delta v\rangle$ and $\langle\delta w\rangle$ is a result of the symmetry about the line joining the centre of the target with the pericentre of the perturber. In this approximation, the z-component of the angular momentum is conserved but the other components are generally altered and the disc is therefore tilted. Since all of the energy changes in our treatment are second order in $\delta\mathbf{v}_s$, they may be underestimates for encounters with $v_p \approx v_c$. A potentially more serious uncertainty is the degree to which collective effects could transport and amplify these energy changes after an encounter. The work of Hunter & Toomre (1969) shows that some of the warping motions induced by the tidal disturbance of a cold, infinitely thin disc are transported outwards. If this is also true of more realistic discs, the thickening at small radii would be overestimated by equation (17).

The response of a warm disc to a tidal disturbance should depend on the stability of its large-scale modes. Toomre (1981) argues that this is controlled by the local parameters $Q \equiv \kappa\,\langle u^2\rangle^{1/2}/3.36\,G\mu$ and $X \equiv R\kappa^2/2\pi mG\mu$ where $\mu\,(R)$ is the surface density at R and m is an azimuthal wavenumber. His analytical and numerical calculations show that the epicyclic energy of a wave is hardly affected for $X \gtrsim 3$ over a wide range in Q. For $X \lesssim 3$, however, it may be amplified in a few revolutions by one or two orders of magnitude depending on the value of Q. A global parameter that appears to control the stability of an exponential disc embedded in a spherical halo is $Y \equiv v_c/(\alpha M_D G)^{1/2}$ where α^{-1} is the scale-radius and M_D is the mass of the disc. The numerical simulations of Efstathiou, Lake & Negroponte (1982) show that bar-like modes are stable for $Y \gtrsim 1.0$ and unstable for $Y \lesssim 1.0$ over a wide range in Q. Sellwood (1983) has shown that the critical value of Y corresponds to the critical value of X at the median radius of an exponential disc. This suggests that the application of our formulae to real galaxies should depend on their stability as measured by either X or Y.

As a check on these arguments, we have simulated a tidal encounter using the two-dimensional Fourier code developed and kindly made available by Efstathiou *et al.* (1982). The unperturbed disc is identical to their model 13, which has 20 000 bodies, $Q = 1.0$ at all radii and $Y = 1.3$; it is therefore more responsive to small-scale modes than it is to large-scale modes. After five revolutions in equilibrium the disc was perturbed by an impulse in the form of equations (19) and (20) with $\theta = \phi = \psi = 45°$, $v_p/v_c = 6$, $\alpha p = 3$ and $M_p/M_d = 4$. The change in the epicyclic energy at that time agreed with the value predicted by equations (15), (23) and (24) and five revolutions later it was a factor of 1.8 higher. We did not consider the simulation of a disc with $Y \lesssim 1.0$ worthwhile because the work of Efstathiou *et al.* shows that it would form a bar and evolve to $Q \approx 2.0$ on its own. The effects of a tidal disturbance would then be hard to distinguish from those of the bar although most of the amplification would probably be suppressed by the increased heat in the disc. Thus, unless purely stellar simulations are a poor guide to the behaviour of real galaxies, our kinematic formulae should be valid at the level of accuracy needed in the applications that follow.

4 Averages over encounters

We first compute the cumulative effects of tidal interactions in an idealized aggregate – a group or cluster – with a uniform density, n_a, of identical galaxies and an isotropic distribution of velocities. As a result of gravitational focusing, the rate of encounters must be determined by the distribution of impact parameters and relative velocities at large separations,

p_∞ and v_∞, respectively. These are related to the corresponding quantities at pericentre by the conservation of energy and angular momentum:

$$v_p^2 - v_e^2(p) = v_\infty^2, \qquad pv_p = p_\infty v_\infty. \tag{26}$$

Then the number of encounters in the time interval $(t, t+dt)$ with orbital parameters in the interval $(p, p+dp)\times(v_p, v_p+dv_p)\times(\theta, \theta+d\theta)\times(\psi, \psi+d\psi)$ is given by

$$\begin{aligned} dN(p, v_p, \theta, \psi) &= (2\pi p_\infty\, dp_\infty)\,(n_a\, v_\infty\, dt)\,(v_\infty^2 F(v_\infty)\, dv_\infty \sin\theta\, d\theta\, d\psi) \\ &= 2\pi n_a\,[v_p^2 + \tfrac{1}{2} p\, dv_e^2(p)/dp]\, F\,([v_p^2 - v_e^2(p)]^{1/2}) p\, dp v_p\, dv_p \sin\theta\, d\theta\, d\psi\, dt \end{aligned} \tag{27}$$

where $4\pi v_\infty^2 F(v_\infty)\, dv_\infty$ is the fraction of pairs with relative velocities in the interval $(v_\infty, v_\infty + dv_\infty)$ and the Jacobian of the transformation (26) has been used for the second equality.

In the computations that follow, we adopt the distribution function

$$F(v_\infty) = (2\pi^{1/2}\sigma_a)^{-3} \exp(-v_\infty^2/4\sigma_a^2). \tag{28}$$

This is based on the standard result that the distribution of relative velocities is Maxwellian with a dispersion $2^{1/2}\sigma_a$ when the distribution of absolute velocities is Maxwellian with a one-dimensional dispersion σ_a (Landau & Lifshitz 1959). If the aggregate is in a steady-state, the average change in any quantity $q(R)$ over the time-interval τ is

$$\begin{aligned} \Delta q(R) = \pi^{1/2}(\tau n_a/\sigma_a^3) &\int_0^\infty dv_p v_p \int_{p_{min}}^{p_{max}} dp p\,[v_p^2 + \tfrac{1}{2} p\, dv_e^2(p)/dp] \\ &\times \exp\{[v_e^2(p) - v_p^2]/4\sigma_a^2\}\, \langle\langle \delta q(R, p, v_p)\rangle\rangle \end{aligned} \tag{29}$$

where the second set of brackets denotes an average over the angles of the encounters:

$$\langle\langle \delta q(R, p, v_p)\rangle\rangle \equiv \frac{1}{4\pi}\int_{\partial\pi}^{\pi} d\theta \sin\theta \int_0^{2\pi} d\psi\, \langle \delta q(R, p, v_p, \theta, \psi)\rangle. \tag{30}$$

After some lengthy manipulations, we find

$$\langle\langle(\delta u)^2\rangle\rangle = \tfrac{1}{15}\Lambda^2(3\Pi^2 - 8\Pi + 8), \tag{31}$$

$$\langle\langle(\delta v)^2\rangle\rangle = \langle\langle(\delta w)^2\rangle\rangle = \tfrac{1}{15}\Lambda^2(\Pi^2 - \Pi + 1). \tag{32}$$

The total changes in the epicyclic and vertical energies are now given by the combination of equations (15), (17), (29), (31) and (32):

$$\Delta E_e(R) = \tfrac{8}{3}\pi^{1/2}(\tau n_a/\sigma_a)\,(v_{cp}^2 r_{Hp})^2 I(R/r_{Hp}, \sigma_a/v_{cp}) \tag{33}$$

$$\Delta E_z(R) = \tfrac{8}{15}\pi^{1/2}(\tau n_a/\sigma_a)\,(v_{cp}^2 r_{Hp})^2 J(R/r_{Hp}, \sigma_a/v_{cp}) \tag{34}$$

$$\begin{aligned} I(R/r_{Hp}, v_{cp}/\sigma_a) \equiv (1.3R/r_{Hp})^2 &\int_0^\infty dx\, x \exp(-\tfrac{1}{4}x^2) \int_{y_{min}}^{y_{max}} dy\, y \\ &\times [1 - 5.2(v_{cp}/\sigma_a)^2 (y/x)^2 (y^2+2)^{-3/2}]\, \exp[2.6(v_{cp}/\sigma_a)^2 (y^2+2)^{-1/2}] \\ &\times \left\{\frac{4y^4}{[y^2+1+\tfrac{2}{3}(1.3R/r_{Hp})^2]^4} - \frac{4y^2}{[y^2+1+\tfrac{2}{3}(1.3R/r_{Hp})^2]^3} + \frac{2}{[y^2+1+\tfrac{2}{3}(1.3R/r_{Hp})^2]^2}\right\} \end{aligned} \tag{35}$$

$$J(R/r_{\mathrm{Hp}}, v_{\mathrm{cp}}/\sigma_{\mathrm{a}}) \equiv (1.3\,R/r_{\mathrm{Hp}})^2 \int_0^\infty dx\, x \exp(-\tfrac{1}{4}x^2) \int_{y_{\min}}^{y_{\max}} dy\, y$$
$$\times [1-5.2\,(v_{\mathrm{cp}}/\sigma_{\mathrm{a}})^2 (y/x)^2 (y^2+2)^{-3/2}] \exp[2.6\,(v_{\mathrm{cp}}/\sigma_{\mathrm{a}})^2 (y^2+2)^{-1/2}]$$
$$\times\left\{\frac{4y^4}{[y^2+1+\tfrac{2}{3}(1.3R/r_{\mathrm{Hp}})^2]^4} - \frac{2y^2}{[y^2+1+\tfrac{2}{3}(1.3R/r_{\mathrm{Hp}})^2]^3} + \frac{1}{[y^2+1+\tfrac{2}{3}(1.3R/r_{\mathrm{Hp}})^2]^2}\right\}. \quad (36)$$

In the derivation of these formulae, we have used the escape velocity given by equation (5), the conversion factors given by equation (11) and set $\kappa = 2^{1/2}\Omega$, as appropriate for galaxies with flat rotation curves. Although equations (33) to (36) are strictly valid only for identical targets and perturbers, we have retained the subscript p to emphasize the dominant effect of the perturbers (see below). The integration variables in equations (35) and (36) are $x = v_{\mathrm{p}}/\sigma_{\mathrm{a}}$ and $y = 1.3p/r_{\mathrm{Hp}}$ and the integration limits correspond to the restriction $p_{\min}(v_{\mathrm{p}}) \leqslant p \leqslant p_{\max}(v_{\mathrm{p}}, R)$ given by conditions (2), (4), (5) and $v_{\mathrm{p}} \geqslant v_{\mathrm{e}}(p)$.

We have examined the contribution of various regimes in Fig. 1 to the dimensionless integrals I and J at $R = 0.5r_{\mathrm{Hp}}$ for $\sigma_{\mathrm{a}} = v_{\mathrm{cp}}$, as in a typical group, and $\sigma_{\mathrm{a}} = 5v_{\mathrm{cp}}$, as in a typical cluster. Adiabatic and merging encounters are negligible in clusters whereas they would increase ΔE_{e} and ΔE_{z} by 50 per cent in groups if they were not excluded. Most of the energy change in both kinds of aggregates is, however, caused by interpenetrating encounters at moderately high velocities. For example, 77–90 per cent is due to collisions with $p \leqslant 3r_{\mathrm{Hp}}$ and 68–98 per cent is due to collisions with $v_{\mathrm{p}} \geqslant 3v_{\mathrm{cp}}$ for velocities in the range $1 \leqslant \sigma_{\mathrm{a}}/v_{\mathrm{cp}} \leqslant 5$. This illustrates the importance of modifying the standard impulse approximation for encounters between galaxies. If we had simply used equation (1) with a cut-off $p_{\min}$ given by equation (3), we would have underestimated the energy changes by a factor of 2 to 5.

The variations of I and J with R/r_{Hp} and $\sigma_{\mathrm{a}}/v_{\mathrm{cp}}$ are shown in Fig. 3. For $\sigma_{\mathrm{a}} \gtrsim 3v_{\mathrm{cp}}$, the integrals have virtually no dependence on velocity and for $\sigma_{\mathrm{a}} \simeq v_{\mathrm{cp}}$ the deviation from

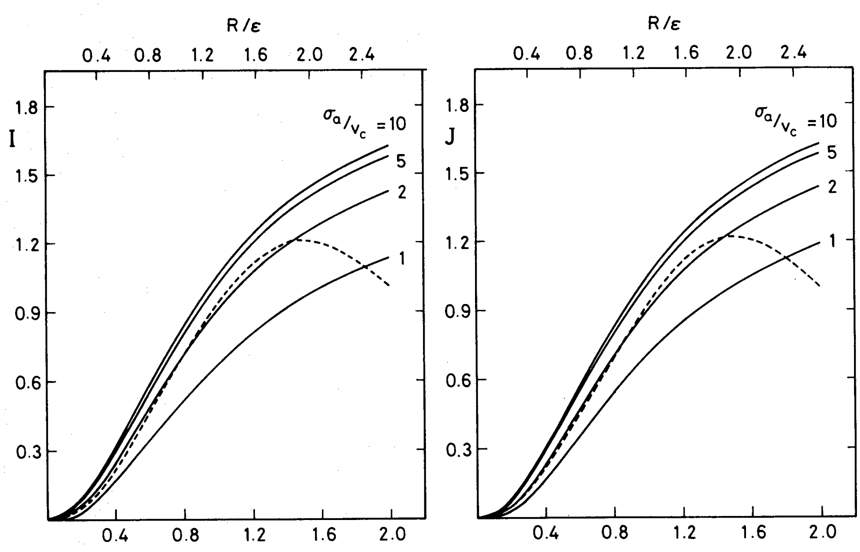

Figure 3. Integrals I and J for tidal energy changes as a function of radial position in the disc and velocity dispersion in the aggregate. The solid lines are from numerical integrations of equations (35) and (36) for identical targets and perturbers and the dashed line is the approximation given by equation (37).

constancy, which is caused by focusing, is only 35 per cent. To the level of accuracy needed in the comparison with observational data, such behaviour can be neglected and this implies that ΔE_e and ΔE_z are nearly proportional to v_{cp}^4/α_a. The radial dependence of I and J can be approximated by the expression

$$I \simeq J \simeq 1.4\,(4)\,(R/r_{Hp})^2 \exp\left[-0.44\,(R/r_{Hp})^2\right] \tag{37}$$

over the range $0 \lesssim R/r_{Hp} \lesssim 1.5$. The functional form of equation (37) was chosen so that the integrations below could be carried out analytically and the coefficients were fitted to the curve with $\sigma_a = 2v_c$, which is typical of the sample discussed in the next section. For $R \gtrsim 1.5 r_{Hp}$, I and J are underestimated by this expression but this part of the range is not important in the applications to centrally concentrated discs.

A simple adaptation of these formulae to an aggregate with a realistic density profile and a spectrum of perturbers is possible if the velocities of galaxies are not correlated with their positions or masses. In this case, n_a must be replaced by $\phi(M_p)\,dM_p/V_{eff}$ where $\phi(M_p)\,dM_p$ is the number of perturbers with masses in the interval $(M_p, M_p + dM_p)$ and the 'effective' volume of the aggregate is defined by

$$V_{eff}^{-1} \equiv \int d^3\mathbf{r}\, n_a^2(\mathbf{r}) \bigg/ \left[\int d^3\mathbf{r}\, n_a(\mathbf{r})\right]^2. \tag{38}$$

This corresponds to a density-weighted average density and accounts for the frequency of binary encounters throughout the aggregate. The effective volume depends sensitively on the central concentration of the aggregate and the energy changes derived with it will be underestimates in the densest regions and overestimates in the sparsest regions. To the extent that focusing is negligible, equations (33) to (36) give the correct energy changes induced in a target with an arbitrary circular velocity and median radius by a perturber with the particular values v_{cp} and r_{Hp} for these parameters. In this case, we can simply integrate the previous expressions for ΔE_e and ΔE_z over $\phi(M_p)\,dM_p$ after expressing v_{cp} and r_{Hp} in terms of M_p.

By analogy with the Schechter (1976) luminosity function with index -1, we assume that the mass function of the perturbers is

$$\phi(M_p) = (fM_a/M^* M_p)\exp(-M_p/M^*) \tag{39}$$

where M^* is a fiducial mass to be specified later, M_a is the total mass of the aggregate and f is the fraction of the mass that is actually attached to the perturbers. The remaining fraction, which is assumed to reside in a smooth background, influences the heating rates only through its effect on the velocity dispersion of the aggregate. By analogy with the Faber–Jackson (1976) and Tully–Fisher (1977) relations, we assume that the median radii and circular velocities of the perturbers scale with their masses as follows:

$$r_{Hp} = r_H^*(M_p/M^*)^{1/2}, \quad v_{cp} = v_c^*(M_p/M^*)^{1/4}. \tag{40}$$

The combination of equations (33), (34), (37), (39) and (40) and an integration over M_p gives our final formulae:

$$\Delta E_e \simeq 4.5\tau\,(fGM_a/V_{eff}\sigma_a)\,(v_c^{*2} r_H^*)\,(R/r_H^*)^3 K_1(1.3\,R/r_H^*), \tag{41}$$

$$\Delta E_z \simeq 0.90\tau\,(fGM_a/V_{eff}\sigma_a)\,(v_c^{*2} r_H^*)\,(R/r_H^*)^3 K_1(1.3\,R/r_H^*), \tag{42}$$

where K_1 is the modified Bessel function of first order.

5 Comparison with observations

To compare the tidal heating computed in the previous section with the energies of unperturbed galaxies, we require a model for their mass distributions. This is assumed to have an exponential radial profile $\mu(R)$ and a vertical profile $\nu(z)$ that is independent of R; thus

$$\rho(R,z) = \mu(R)\,\nu(z) = (M_D\alpha^2/2\pi)\exp(-\alpha R)\,\nu(z) \tag{43}$$

where M_D and α^{-1} are respectively the total mass and the scale-radius of the disc. In this case, the projected density of an edge-on galaxy also separates into a radial factor time $\nu(z)$, consistent with the photometry of van der Kruit & Searle (1981a, b). For the vertical profiles of discs with thin and thick components, we introduce a family of models in parametric form

$$\nu(z) = \frac{1}{2\beta}\,\mathrm{sech}^{2+\gamma}\xi, \qquad z = \pm\beta\int_0^{\xi} d\xi'\cosh^{\gamma}\xi' \tag{44}$$

where the constants β and γ specify the normalization and the shape of the mass distribution. This model is a generalization of the familiar isothermal sheet, which corresponds to $\gamma = 0$ and fits the observed profiles of thin discs (van der Kruit & Searle 1981a, b). As Fig. 4 shows, larger values of γ correspond to composite profiles with greater proportions of their mass in the thick component.

The internal energy of this model can be computed from the gravitational acceleration in the vertical direction, $K(z)$. Using equations (43) and (44) and Poisson's equation for a plane-stratified sheet, we find

$$K(z) = \mp 2\pi G\mu \tanh\xi. \tag{45}$$

The potential energy per unit area and mass of the disc is therefore

$$W_z = -\int_{-\infty}^{+\infty} dz\, z\,\nu(z)\,K(z) = \pi G\mu\beta\int_0^{\infty} d\xi\,\mathrm{sech}^{2-\gamma}\xi$$
$$= 1/2\,\pi^{3/2}G\mu\beta\Gamma(1-\gamma/2)/\Gamma(3/2-\gamma/2) \tag{46}$$

for $\gamma < 2$, where Γ denotes the usual gamma function. When γ exceeds 2, the energy diverges unless the profile is truncated at some finite z. As a means of comparing different profiles,

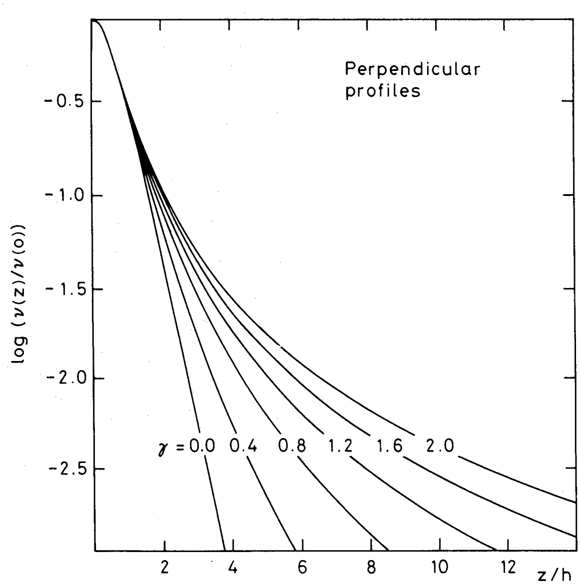

Figure 4. Perpendicular profiles for the family of models defined by equations (44) and (47). The parameter γ determines the relative prominence of thin and thick disc components for a fixed scale-height h.

we define a 'scale-height' for the thin component of a disc,

$$h \equiv \beta/(1+\gamma/8). \tag{47}$$

To an accuracy of a few per cent, this is the distance at which the density has dropped to $\mathrm{sech}^2(1)=0.42$ of its value in the midplane. (Equation 47 therefore differs from the standard definition of a scale-height.) The ratio of the energy of a disc with $0 \leqslant \gamma < 2$ to one with $\gamma = 0$ and the same values of h, α^{-1} and M_D is then

$$\frac{\Delta W_z}{W_z} = (\pi^{1/2}/2)\,(1+\gamma/8)\,\frac{\Gamma(1-\gamma/2)}{\Gamma(3/2-\gamma/2)} - 1. \tag{48}$$

We now return to the energy changes induced by tidal interactions. These should increase outwards in the disc but the exact radial dependence is difficult to predict because of uncertainties in the transport by collective effects. In any case, it is convenient to have global estimates of $\Delta E_e/E_e$ and $\Delta E_z/E_z$ for comparison with the observations. We therefore integrate equations (41) and (42) over the disc specified by equation (43):

$$\Delta E_e = 124\tau\,(fGM_a/V_{\mathrm{eff}}\sigma_a)\,(v_c^{*2}M_D/\alpha)\,g(s), \qquad \Delta E_z = {}^1\!/_5\,\Delta E_e \tag{49}$$

$$g(s) = \frac{s^3}{(1+s)^6}\,F\left(6, \frac{3}{2}; \frac{11}{2}; \frac{1-s}{1+s}\right), \qquad s \equiv 1.33/\alpha r_H^* \tag{50}$$

where F is Gauss' hypergeometric function (see Gradshteyn & Ryzhik 1980, equation 6.621.3). These energy changes are to be compared with the epicyclic and vertical energies in the corresponding unperturbed disc, which is assumed to have $\gamma = 0$ and values of Q, h and Ω_c that are independent of R. An integration over equations (14) and (16) with the use of equation (46) gives

$$E_e = (3.36^2/108\pi^2)\,(Q^2\alpha^2/v_c^2)\,G^2M_D^3. \tag{51}$$

$$E_z = {}^3\!/_{16}\,hGM_D^2\alpha^2. \tag{52}$$

The fractional energy changes are therefore

$$\Delta E_e/E_e = 1.17\times 10^4\,\tau\,(fGM_a/V_{\mathrm{eff}}\sigma_a)\,(v_c^*/v_c)^2\,(Y^2/Q)^2\,g(s)/\alpha \tag{53}$$

$$\Delta E_z/E_z = 132\tau\,(fGM_a/V_{\mathrm{eff}}\sigma_a)\,(v_c^*/v_c)^2\,Y^2(\alpha h)^{-1}g(s)/\alpha \tag{54}$$

where Y is the dimensionless parameter defined in Section 3.

These expressions for $\Delta E_e/E_e$ and $\Delta E_z/E_z$ are independent of the distance scale but we find it convenient to assume a Hubble constant of $H_0 = 100\ \mathrm{km\ s^{-1}\ Mpc^{-1}}$ in their evaluation. Thus the age of any aggregate is taken to be $\tau = H_0^{-1} = 10\times 10^9$ yr. For the fiducial circular velocity we adopt $v_c^* = 230\ \mathrm{km\ s^{-1}}$, which is typical of galaxies with luminosities near $L^* = 6.6\times 10^9\,L_\odot$ [on the $B(0)$ system used by Huchra & Geller 1982; see below]. Although the corresponding median radius is not directly observable and may depend on environment, it can be related to the fraction of the mass that is attached to galaxies in the aggregate under consideration; thus

$$r_H^* = GM^*/2v_c^{*2} = G\,(fM_aL^*/L_a)/2v_c^{*2} = 0.27\,f\,(M_a/L_a)_\odot\ \mathrm{kpc}. \tag{55}$$

This expression and the condition that the dark haloes of galaxies be at least as large as their visible bodies, imply the range $0.1 \lesssim f \lesssim 1.0$ for typical values of M_a/L_a. Without making any commitments about the stability of disc galaxies, we adopt $Q = 2.0$ and $Y = 1.0$ because the

Table 1. Data for edge-on galaxies and their parent groups.

NGC	Type	Group	σ_a/km s^{-1}	$M_a/M_\odot$	$(M_a/L_a)_\odot$	V_{eff}/Mpc^3	v_c/km s^{-1}	α^{-1}/kpc	αh	γ	$\Delta W_z/W_z$	$\Delta E_z/E_z$	$\Delta E_e/E_e$
891	Sb	N1023/67	120	5.4E12	520	0.32	225	3.2	0.20	1.1	>0.3 <0.9	0.05	0.2
4111	S0	CVnII/60	120	6.5E12	120	7.0	170	1.2	0.33	1.5	>0.3 <2	0.002	0.01
4244	Scd	CVnI/60	90	1.5E13	330	27	106	3.3	0.22	0.0	0.0	0.01	0.07
4350	S0	Virgo/41	620	2.2E14	190	4.2	200	1.2	0.41	2.5	>0.4	0.007	0.06
4474	S0	Virgo/41	620	2.2+14	190	4.2	170	1.2	0.62	>3	>0.4	0.006	0.08
4570	S0	Virgo/41	620	2.2E14	190	4.2	210	1.6	0.39	1.8	>0.4 <6	0.01	0.1

Notes

The source for the morphological types is the *Second Reference Catalogue* (de Vaucouleurs, de Vaucouleurs & Corwin 1976). Apart from V_{eff}, all parameters for the Virgo cluster and the N1023 group were taken from Huchra & Geller (1982). Those for CVnI and CVnII, which are subgroups of HG60, were computed by the same procedure using the membership assignments by de Vaucouleurs (1975). Our procedure for estimating V_{eff} is described in the text. The value of v_c for NGC 891 is from Sancisi & Allen (1979) and that for NGC 4244 is from Sancisi (quoted by Bosma 1981). Since no kinematic data are available for the lenticulars we have estimated v_c from the total luminosities and the mean relation $v_c/v_c^* \simeq (L/L^*)^{1/4}$. The values of α^{-1}, h and γ for the spirals are based on the photometry by van der Kruit & Searle (1981a, b) and those for the lenticulars are based on the photometry by Burstein (1979a, b, c). In most cases, these were estimated by eye from the published profiles as described in the text. Equation (44) is a poor fit to the perpendicular profiles of NGC 4474 and γ could only be assigned a rough lower limit. All distance-dependent quantities are based on the mean radial velocities of the groups, a far field Hubble constant of 100 km s^{-1} Mpc^{-1} and a Virgocentric infall velocity of 300 km s^{-1}. The values of $\Delta W_z/W_z$, $\Delta E_z/E_z$ and $\Delta E_e/E_e$ were computed from equations (48), (50), (53), (54) and (55) with the parameters tabulated above or specified in the text.

observational evidence suggests that these values are approximately correct (Fall & Efstathiou 1980; Efstathiou *et al.* 1982).

The remaining parameters needed in the computation of ΔE_e and ΔE_z are summarized in Table 1 for six edge-on galaxies. These have surface photometry by Burstein (1979a, b, c) or van der Kruit & Searle (1981a, b) and membership in the group catalogue compiled by Huchra & Geller (1982). A complete description of the sources of the data and the procedure used to estimate the parameters is given in the notes to the table. The NGC numbers and morphological types of the galaxies are listed in columns 1 and 2 and the names, line-of-sight velocity dispersions, virial masses and mass-to-light ratios of their parent groups are listed in columns 3–6. The effective volumes of the groups, given in column 7, are based on a form of equation (38) in which the spatial density profile $n_a(r)$ is expressed in terms of the projected density profile by means of von Zeipel's formula (see, for example, Mihalas & Routly 1968, section 14.3). To estimate $V_{\rm eff}$, we then used the counts of galaxies in concentric rings on the sky and replaced the integrals over the groups by discrete sums. The effective volume derived in this way for the Virgo cluster is quite stable but the values derived for the other groups are affected by small numbers and are only reliable at the 50–100 per cent level.

The circular velocities, scale-radii, scale-heights and γ values of the galaxies in this sample are listed in columns 8 to 11 of Table 1. An average value of h and an average value of γ were estimated by comparing the model profiles shown in Fig. 4 with the observed profiles between radii of α^{-1} and $4\alpha^{-1}$. For galaxies with $\gamma < 2$, the value of $\Delta W_z/W_z$ that would be required to produce the thick discs from their thin discs could be computed directly from equation (48). Since this is based on integrations of $\nu(z)$ to $|z| \to \infty$, the results are upper limits. We also obtained lower limits by truncating the integrations at $|z| = 5h$, which is where the observed profiles usually disappear into the noise. These estimates are listed in column 12 and the tidal changes in the vertical and epicyclic energies given by equations (53) and (54) with $f = 1.0$ are listed in columns 13 and 14. Although this value of f is extreme, reducing it to 0.1 would only decrease $\Delta E_z/E_z$ and $\Delta E_e/E_e$ by factors of 1.5 to 3 for the galaxies in our sample.

The results presented in Table 1 suggest that tidal heating is a small effect in the Virgo cluster and nearby groups. In all cases, the predicted changes in the epicyclic energies are an order of magnitude smaller than the corresponding energies inferred for the unperturbed discs. Even smaller changes are predicted for the vertical energies and in no case are they within an order of magnitude of the values needed to explain the formation of thick discs by this mechanism. Considering the uncertainties in all of the parameters except f that enter equations (53) and (54), we estimate that $\Delta E_e/E_e$ and $\Delta E_z/E_z$ are uncertain by factors of about 3. This is roughly consistent with the dispersion in our small sample so that no clear dependence on environment could be expected to emerge from it. Since we have generally been conservative in the choice of parameters, the energy changes given in Table 1 are more likely to be systematically high than they are to be low in the absence of collective effects. In the case that the discs are stabilized by their haloes, these values should probably be doubled to account for the amplification neglected by our kinematic formulae.

6 Discussion and conclusions

The results of the previous section suggest that tidal interactions are weak in the environments where disc galaxies are most common. Since the heating rates scale approximately with the mass, effective volume and velocity dispersion of an aggregate as $M_a/V_{\rm eff}\sigma_a$, they should be highest in rich clusters with large central concentrations. For the Coma cluster, Rood *et al.* (1972) estimate $M_a \approx 3 \times 10^{15} M_\odot$ and $\sigma_a \approx 900 \text{ km s}^{-1}$ and from their fitted density profiles, we compute $V_{eff} \approx 3.0 \text{ Mpc}^3$. The predicted energy changes are therefore about 10 times higher on average in Coma than they are in Virgo for reasonable values of the fraction of mass attached to galaxies in the two clusters ($0.1 \lesssim f \lesssim 1.0$). This implies $\Delta E_e/E_e \sim 1$ and $\Delta E_z/E_z \sim 0.1$ for typical spirals and lenticulars in Coma with the parameters adopted in Section 5. Considering the uncertainties inherent in our treatment, the interpretation of these average energy changes is slightly ambiguous. They probably imply that tidal heating plays a significant role in the evolution of some members of the Coma cluster, especially those that spend most of their time in the core. Since this is an extreme, albeit interesting case, it does not alter our conclusions about the majority of disc galaxies.

The analytic formalism developed here has the advantage over numerical simulations that it can be adapted to a variety of circumstances with little effort. Another point in favour of our method is that it does not suffer from the low resolution and the internal relaxation typical of disc models with ~1000 bodies. Nevertheless, the present analytic treatment neglects several effects, such as resonant stars, bound companions and halo deformations, which are more amenable to direct numerical treatment. By ignoring these effects, we have assumed implicitly that they are only important for the encounters that eventually lead to merging. A more serious concern is the amplification of the energy changes in a disc by collective effects after an encounter. With a 20 000-body simulation, we have shown that our kinematic formulae are correct to within a factor of 2 if the disc is stabilized by a halo ($Y \gtrsim 1.0$). Furthermore, we have argued that a disc without such a halo would develop a bar and generate enough epicyclic motion on its own to suppress collective effects ($Q \approx 2.0$). The last point is, however, conjectural and our predicted energy changes might have to be increased substantially if the old stellar populations of disc galaxies can somehow be kept in unstable states for long periods.

Our results show that most of the tidal heating is caused by interpenetrating encounters with velocities a few times higher than the circular velocities of the discs. We find that, short of merging, the cumulative effects of tidal interactions are not sufficient to alter the gross structural and kinematical properties of most disc galaxies. Some other mechanism is therefore required to produce thick discs and the most likely explanation may be in terms of flattened bulges. Moreover, tidal heating is unlikely to suppress instabilities in spirals as a means of converting them into lenticulars. We emphasize that these conclusions are based on a statistical treatment and they do not rule out the importance of tidal interactions in exceptional cases. Our results suggest that, if the present environment of galaxies plays a significant role in determining their morphologies, it does so mainly through interactions with their gaseous parts. Alternatively, the influence of the environment may have been much stronger at very early times when galaxies, groups and clusters were in the process of formation.

Acknowledgments

We thank Drs G. Efstathiou, D. Lynden-Bell, J. A. Sellwood, A. Toomre and S. D. M. White for helpful discussions. OEG is grateful to the Dr Carl Duisberg-Stiftung and to the Studientstiftung des Deutschen Volkes for financial support.

References

Aarseth, S. J. & Fall, S. M., 1980. *Astrophys. J.*, **236**, 43.
Alladin, S. M., 1965. *Astrophys. J.*, **141**, 768.
Bosma, A., 1981. *Astr. J.*, **86**, 1825.

Bothun, G. O. & Sullivan, W. T., 1980. *Astrophys. J.,* **242,** 903.
Burstein, D., 1979a. *Astrophys. J. Suppl.,* **41,** 435.
Burstein, D., 1979b. *Astrophys. J.,* **234,** 435.
Burstein, D., 1979c. *Astrophys. J.,* **234,** 829.
Camm, G. L., 1967. In *Colloque les Nouvelles Methodes de la Dynamique Stellaire,* p. 141. CNRS, Paris.
Dekel, A., Lecar, M. & Shaham, J., 1980. *Astrophys. J.,* **241,** 946.
de Vaucouleurs, G., 1975. In *Galaxies and the Universe,* p. 557. eds Sandage, A., Sandage, M. & Kristian, J., University of Chicago Press, Chicago.
de Vaucouleurs, G., de Vaucouleurs, A. & Corwin, H. G., 1976. *Second Reference Catalogue of Bright Galaxies,* University of Texas Press, Austin.
Dressler, A., 1980. *Astrophys. J.,* **236,** 351.
Efstathiou, G., Lake, G. & Negroponte, J., 1982. *Mon. Not. R. astr. Soc.,* **199,** 1069.
Faber, S. M. & Jackson, R. E., 1976. *Astrophys. J.,* **204,** 668.
Fall, S. M. & Efstathiou, G., 1980. *Mon. Not. R. astr. Soc.,* **193,** 189.
Farouki, R. T. & Shapiro, S. L., 1981. *Astrophys. J.,* **243,** 32.
Freeman, K. C., 1980. In *Photometry, Kinematics and Dynamics of Galaxies.* p. 85. ed. Evans, D. S., University of Texas Press, Austin.
Gerhard, O. E., 1981. *Mon. Not. R. astr. Soc.,* **197,** 179.
Gradshteyn, I. S. & Ryzhik, I. M., 1980. *Table of Integrals, Series and Products,* Academic Press, New York.
Huchra, J. P. & Geller, M. J., 1982. *Astrophys. J.,* **257,** 423.
Hunter, C. & Toomre, A., 1969. *Astrophys. J.,* **155,** 747.
Knobloch, E., 1976. *Astrophys. J.,* **209,** 411.
Knobloch, E., 1978. *Astrophys. J. Suppl.,* **38,** 253.
Kormendy, J. & Norman, C. A., 1979. *Astrophys. J.,* **233,** 539.
Landau, L. D. & Lifshitz, E. M., 1959. *Statistical Physics,* Pergamon Press, London.
Lindblad, B., 1959. In *Handbuch der Physik,* Vol. 53, p. 21. ed. Flugge, S., Springer Verlag, Berlin.
Marchant, A. B. & Shapiro, S. L., 1977. *Astrophys. J.,* **215,** 1.
Mihalas, D. & Routly, P. M., 1968. *Galactic Astronomy,* Freeman, New York.
Richstone, D. O., 1975. *Astrophys. J.,* **200,** 535.
Richstone, D. O., 1976. *Astrophys. J.,* **204,** 642.
Rood, H. J., Page, T. L., Kintner, E. C. & King, I. R., 1972. *Astrophys. J.,* **175,** 627.
Sancisi, R. & Allen, R. J., 1979. *Astr. Astrophys.,* **74,** 73.
Schechter, P., 1976. *Astrophys. J.,* **203,** 297.
Sellwood, J. A., 1983. In *Internal Kinematics and Dynamics of Galaxies,* p. 197, ed. Athanassoula, E., Reidel, Dordrecht, Holland.
Spitzer, L., 1958. *Astrophys. J.,* **127,** 17.
Toomre, A., 1981. In *The Structure and Evolution of Normal Galaxies,* p. 111. eds Fall, S. M. & Lynden-Bell, D., Cambridge University Press.
Toomre, A. & Toomre, J., 1972. *Astrophys. J.,* **178,** 623.
Tsikoudi, V., 1979. *Astrophys. J.,* **234,** 842.
Tsikoudi, V., 1980. *Astrophys. J. Suppl.,* **43,** 365.
Tully, R. B. & Fisher, J. R., 1977. *Astr. Astrophys.,* **54,** 661.
van den Bergh, S., 1976. *Astrophys. J.,* **206,** 883.
van der Kruit, P. C. & Searle, L., 1981a. *Astr. Astrophys.,* **95,** 105.
van der Kruit, P. C. & Searle, L., 1981b. *Astr. Astrophys.,* **95,** 116.